Nonlinear optics in multipass cells

Marc Hanna, Florent Guichard, Nour Daher, Quentin Bournet, Xavier Délen, Patrick Georges*

Marc Hanna, Nour Daher, Xavier Délen, Patrick Georges
Université Paris-Saclay, Institut d'Optique Graduate School, CNRS, Laboratoire Charles Fabry, 91127, Palaiseau, France.
E-mail: marc.hanna@institutoptique.fr

Florent Guichard, Quentin Bournet
Amplitude, 11 Avenue de Canteranne, Cité de la Photonique, 33600 Pessac, France.

Keywords: nonlinear optics, ultrafast optics, pulse compression

We review the fundamental principles and experimental implementations of multipass cells used as a platform for nonlinear optics. Embedding a nonlinear medium in a multipass cell allows for a distribution of the nonlinearity over large interaction distances, while the beam goes through multiple foci, conferring on the beam a robustness with respect to spatio-spectral coupling effects. Most of the research so far has been focused on temporal compression based on self-phase modulation, with excellent performances especially in terms of energy scaling and throughput. However, other nonlinear phenomena and functions are being increasingly investigated, such as supercontinuum generation, spectral compression, or Raman scattering. Nonlinear optics experiments in multipass cells bear some similarities with the work done in optical fibers over several decades, while allowing straightforward energy scaling potential, and unlocking engineering possibilities through the design of the cell mirrors, geometry, and nonlinear medium.

1. Introduction

Investigated since the first realization of the laser in 1960, the field of nonlinear optics has grown to become one of the most important areas of photonics,[1] both for the fundamental understanding of light-matter interaction and for scientific and societal applications. Nonlinear propagation effects scale with the optical intensity, and are therefore ubiquitous in

the understanding and development of ultrafast optics, where peak powers are high even at modest pulse energy. In particular, research in novel ultrafast sources is intertwined with the understanding of nonlinear optical phenomena that now constitute a major component of the technological toolkit in ultrafast optics. Notable examples include wavelength conversion through harmonic generation[2] or parametric amplification,[3] temporal[4] or spectral[5] compression using self-phase modulation (SPM), pulse cleaning using cross-polarized wave generation,[6] synchronization through the use of optical Kerr gates,[7] supercontinuum generation,[8] and XUV and attosecond sources using high-harmonic generation.[9]

Although the fundamentals of nonlinear optics have been discovered with beams propagating in free space, optical waveguides and in particular optical fibers have played a major role in the expansion of applications.[10] The reason for this importance is twofold. First, optical fibers spatially confine the field in the core over almost arbitrary interaction lengths, which makes the realm of nonlinear optics accessible to much lower pulse energies / average powers. Second, for single transverse mode structures, the guiding action fixes the spatial properties of the interacting beams. This allows large levels of nonlinearity, while what can be seen as detrimental spatial effects, such as self-focusing or the appearance of spatio-temporal couplings, can be avoided. Although a highly localized spatial mode can be an advantage to exploit nonlinearity at low pulse energy levels, it turns into a drawback to scale the energy of nonlinear subsystems. As a consequence, a large amount of research work has been devoted to devising single transverse mode guiding structures with low nonlinearity, to retain control over the spatial profile of high energy pulses that nonlinearly interact with matter inside the waveguide. This work includes the design of large mode area fibers,[11] large and hollow gas-filled core fibers with advanced guiding mechanisms such as Kagome[12] and antiresonant cladding structures,[13] and gas-filled capillaries:[14] gases exhibit a nonlinear index that is typically three orders of magnitude lower than solids.

In this quest for the ideal implementation of nonlinear optical effects, a trend appeared recently to go back to free-space beam interaction with the nonlinear medium, illustrated in **Figure 1**. Various strategies are employed to avoid excessive spatio-temporal couplings in the output beam: experiments where filamentation occurs can result in a rather homogeneous and spatio-temporally localized wavepacket.[15] Another method consists in arranging the nonlinear interaction in several stages, with linear free-space propagation between stages. An example of this concept is multiplate compression, where several slabs of nonlinear medium are carefully distributed around one or more foci of the propagating beam.[16, 17] By limiting the nonlinearity at each stage, this interaction geometry can keep the spatio-temporal couplings under control.

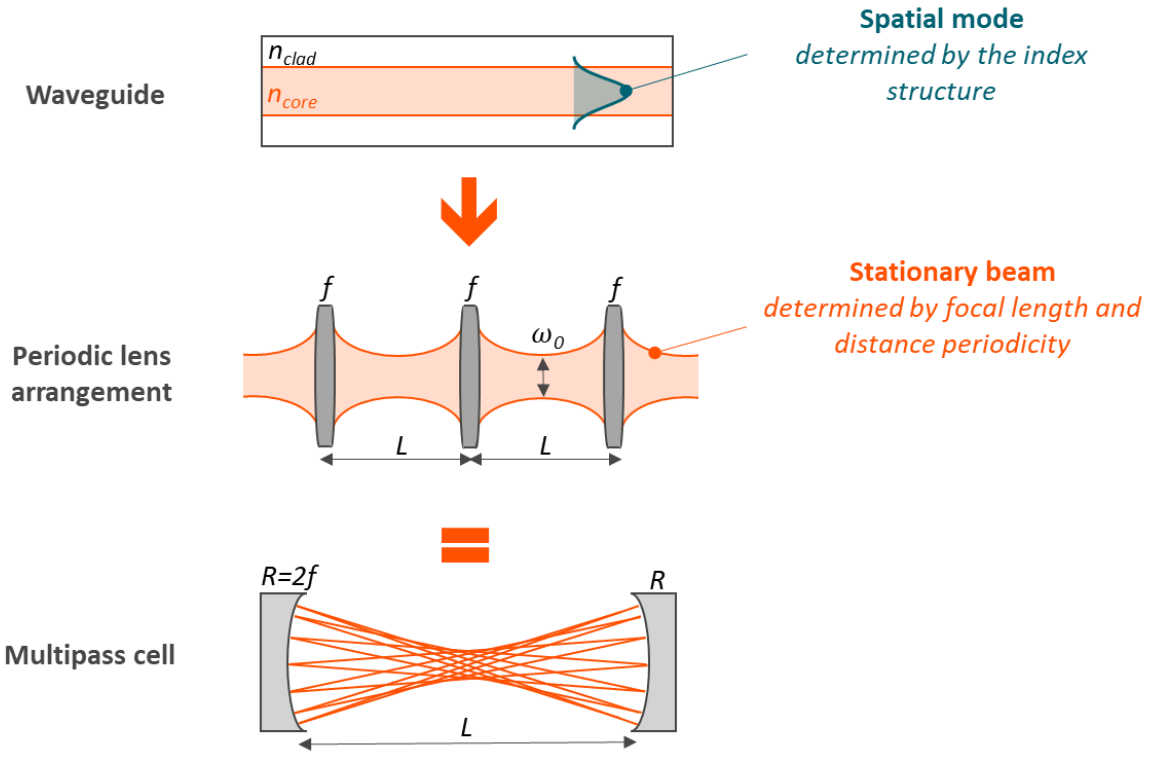

Figure 1. From waveguides to multipass cells as a platform for nonlinear optics.

Recently, a number of experiments were conducted to extend this idea of distributing the nonlinearity over a large free-space propagation distance and a large number of foci: a nonlinear medium is inserted inside a recirculating cell. In addition to resulting in mostly

homogeneous beams, this principle allows a lot of experimental possibilities in terms of the nonlinear material used (solid or gas), dispersion engineering, and energy scaling. In this article, we review the basic principles, design rules, and results obtained in nonlinear optics in multipass cells (MPCs).

One of the first work pointing towards this principle,[18] published in 2000, uses coupled-mode theory to establish the relative robustness of a Gaussian beam propagating through its focus in a mildly nonlinear homogeneous medium. The authors explicitly mention the fact that the use of a MPC would allow to obtain a large B-integral, defined as the maximum phase shift accumulated through SPM, while leaving the spatial profile mostly Gaussian. This idea was not pursued experimentally for the next 15 years, although a couple of theoretical papers[19, 20] examined the use of a periodic nonlinear optical system to compress high intensity femtosecond lasers. The first experimental implementation of a MPC including nonlinear plates was reported in 2016,[21] and demonstrated the advantages of the method, especially in terms of energy throughput. A patent associated to this publication[22] describes a number of important theoretical results and design guidelines. A theoretical analysis of these systems, including numerical simulations of the propagation, along with the proposal to use gas-filled MPCs to scale the pulse energies that can be manipulated, followed in 2017.[23] Since then, a large number of results were reported in vastly different regimes in terms of optical pulse energies and durations.

This article is organized as follows. Section 2 introduces the general notions that are useful to understand operation of nonlinear MPCs, including properties of linear Herriott cells, design of MPCs with solid plates of nonlinear media, and the description of gas-filled MPCs. It ends with a roundup of numerical methods that were used to simulate the propagation of optical pulses in such systems. Section 3 reviews experimental results obtained in nonlinear MPCs for their main application, temporal compression. Finally, section 4 opens up the scope by describing a number of other applications, or different nonlinear effects observed in MPCs.

2. General notions

2.1. Herriott cells

Multipass cells can be seen as optical resonators that are used off-axis,[24] which results in rays that are trapped in the vicinity of the optical axis of the stable periodic optical system. The Herriott cell is the most used geometry, and is formed by two concave mirrors with identical radius of curvature R, separated by a distance $L < 2R$, as depicted in **Figure 2**. It was recognized early on that upon launching an optical ray off-axis in such a system, the distribution of spots on the mirrors forms an elliptical pattern. For particular launching angles and cell geometries, the path can be closed, meaning that the ray return upon themselves after a certain number of roundtrips.

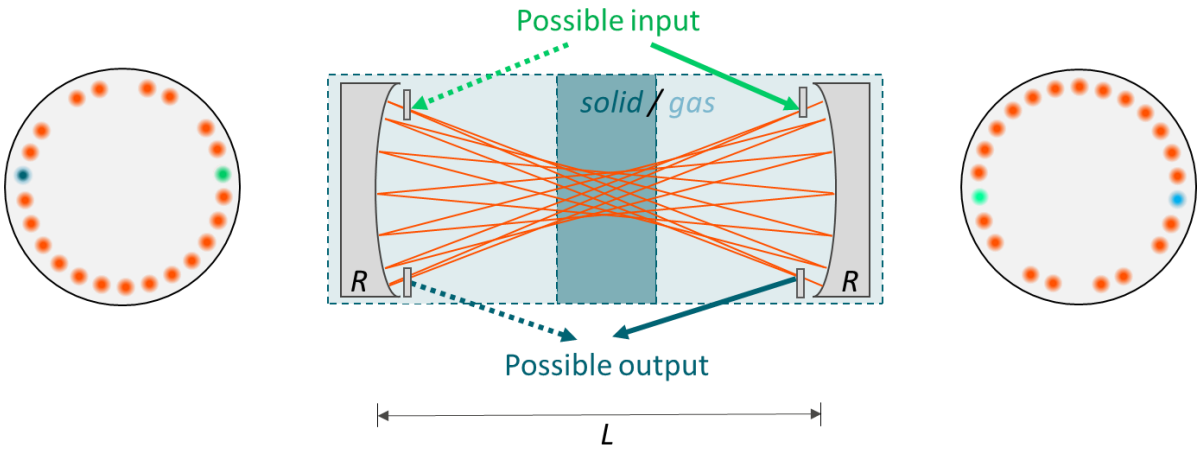

Figure 2. Schematic layout of a nonlinear MPC. The nonlinear medium is either a bulk slab inserted inside the cell (dark blue) or a gas surrounding the cell (light blue). Left and right: a typical arrangement of spots on MPC mirrors for 22 roundtrips in a near concentric MPC, with $L/2\times R$ = 0.9675. The green and blue dots are the first and last passes, allowing convenient injection / extraction of the beam on either side of the cell.

Although such cells can be used in closed-path configuration to mimic a much longer coherent optical resonator, MPCs have also been used in non-interferometric ways to introduce a large propagation distance in a compact configuration. This has been very useful for a number of applications: as an optical delay line,[25] to increase the interaction length in

absorption spectroscopy,[26] or inserted inside modelocked laser cavities to decrease the repetition rate / increase the pulse energy.[27] Nonlinear MPCs are based on such a non-interferometric use, the main idea being that the beam interacts with the nonlinear medium inside the cell over a large number of passes / foci, to distribute the nonlinearity in small increments. The beam must be aligned on a path for which the spot pattern does not overlap, so that it is possible to inject and extract the beam with small mirrors that do not intersect the beam path inside the cell, or through holes in the cell mirror.

In terms of Gaussian beam propagation, for a given MPC geometry determined by *R* and *L*, there exists a beam waist located at the cell middle point for which the beam size and radius of curvature evolution is periodic over one roundtrip. This beam is the same for laser resonators, with a radius at the waist given by

$$w_0 = \sqrt{\frac{\lambda L}{2\pi}\sqrt{\frac{2R}{L} - 1}}, \qquad (1)$$

where λ is the central wavelength. This beam expands upon propagation to a radius at the cell mirror:

$$w_M = w_0\sqrt{\frac{2R}{2R-L}}. \qquad (2)$$

Matching the input beam to this condition ensures to first order that nonlinearity accumulates homogeneously over the roundtrips in the MPC, and that the beam size at the mirrors remains approximately constant. This explains that all experimental efforts have tried to achieve this condition.

In real implementations of nonlinear MPCs, deviations of the input beam from the resonator eigenmode, or modification of its properties due to nonlinear refraction can cause the propagating beam to deviate significantly from the stationary beam. It can be shown[28] that a periodic optical system that is not ideally mode-matched will result in beam parameters that oscillate upon propagation, with a period of oscillation that depends on the accumulated Gouy

phase upon one pass in the optical system. If the effect of the nonlinearity can be accurately described by either a nonlinear lens or a modified nonlinear Gaussian beam, this conclusion holds true for nonlinear MPCs. As a consequence, propagation through the nonlinear periodic optical system results in oscillations of the beam parameters over the successive passes. The amplitude of these beam parameter oscillations depends on the mismatch between the input condition and the eigenmode of the MPC modified by the nonlinearity. In practice this results in optical systems that are quite robust to moderate mismatch and fluctuations of the input beam parameter. Of course this is not valid if the nonlinearity is so strong that it makes the elementary optical system unstable.

The properties of stable periodic optical systems also explain their robustness with respect to input beam pointing fluctuations. By definition of a stable system, an optical ray that is launched at a small angle and/or with a shift in position with respect to the optical reference axis defined by the ideal ray remains in the vicinity of this axis. The angle and position deviation of such an imperfect input ray at each roundtrip through the system depends on the geometric configuration and can easily be calculated using an ABCD matrix approach. In practice, the tolerance of a system to beam pointing fluctuations is also determined by the maximum size of the mirrors that are used to inject/extract the beam inside the cell. This size is related to the spot density on the mirror, and hence to the number of roundtrips. As a consequence there is a design tradeoff between the number of roundtrips and the tolerance to beam pointing fluctuations. This tolerance is a distinct advantage compared to gas-filled capillaries that are also used to perform nonlinear compression.

For MPCs designed so that propagation inside the cell is almost over one closed path, the output beam can be the same as the input beam, regardless of matching to the stationary condition defined in Equation (1) and (2). This is denoted as a “q-preserving” configuration, in reference to the q-parameter that completely defines a Gaussian beam.[29]

A linear input polarization state was shown to be mostly preserved in MPCs, because of the very low incidence angle on the mirrors observed in most practical cases.[30] The successive reflections on the mirrors at angles that are small but nonzero can be shown[30] to result in a rotation of the linear polarization state by an angle given by

$$\alpha = 4N_{rt}\frac{AB}{L^2}\sin^2\frac{\theta}{2}\sin\theta, \qquad (3)$$

where N_{rt} is the number of roundtrips, A and B are the lengths of the long and short half-axes of the ellipse formed by the spot pattern, and $\theta = \arccos(1 - L/R)$. In practical implementations this rotation angle is small.

Herriott cells have been almost exclusively used for nonlinear optics experiments, at the exception of one experiment performed using a White cell in 4f geometry. [31] The Herriott cell results in a simple and predictable spot pattern and relative ease of alignment. However, as the pulse energy and beam size on the cell mirrors increases, the benefits of using single, large diameter curved mirrors decrease compared to the use of multiple small mirrors at each reflection, a more cost-effective solution. High energy MPCs are being designed along this idea, [32, 33] that also makes the spot pattern at each end of the MPC arbitrary, resulting in possibly more compact setups in the transverse direction with respect to light propagation.

2.2. Nonlinear MPCs including plates

A simple way to add optical nonlinearity to a recirculating cell consists in inserting a plate of solid material inside a MPC built in the laboratory in ambient air or inside a vacuum or sealed chamber. It can be seen as an extension of the multiplate concept[16] with a more distributed nonlinearity. Because the nonlinearity per pass through each plate is much smaller, the introduced Kerr lens can be treated as a perturbation to the linear periodic caustic in MPCs, while refocusing effects caused by Kerr lensing in multiplate setups is an essential part of the physics and optimization procedure.

A bulk plate-based MPC was the approach taken for the first demonstration of the idea,[21] where the plates were in fact the fused silica substrates of the MPC mirrors. Given that the nonlinear index of bulk materials is typically three orders of magnitudes larger than that of air, for slab thicknesses of a few millimeters inserted in MPCs with a length below 1 m, the nonlinearity can be considered to originate mostly from the solid material. In this case, if the beam propagation is stationary over a roundtrip, and for given input pulse parameters, the level of nonlinearity solely depends on the beam size in the plate and its thickness. For experiments aimed at accumulating SPM, the amount of nonlinearity experienced by an optical pulse propagating in the device can be quantified by the B-integral:

$$B = \frac{2\pi}{\lambda} \int n_2 I_{peak} dz, \qquad (4)$$

where n_2 is the nonlinear index of the medium and I_{peak} is the peak intensity. It is well known that the amount of B-integral per pass in a plate (e. g. a vacuum chamber window, or a laser crystal) is limited in ultrafast optics experiments by the tolerable amount of space-time couplings in the output beam to practical values below 1 rad. MPCs are no exception, and this condition determines the minimum number of roundtrips that must be achieved for an overall target B-integral. However, unlike systems where the beam propagates in a homogeneous medium such as optical fibers, the peak power is not limited by the critical power: as long as the self-focusing distance is much greater than the plate length, the beam exits the nonlinear medium well before significant changes to the beam are imparted by nonlinear refraction. In practice, pulses with peak powers more than ten times the critical power of the nonlinear medium have been used successfully.[21, 34] The Kerr lens associated with nonlinear refraction causes oscillatory deviations from the linear stationary caustic of the system, that can be reduced either by taking into account the Kerr lens at the design stage, or by experimentally modifying the input beam to approach the nonlinear eigenmode and reduce the observed modifications in beam size at each pass.

One very important parameter in experiments is the energy throughput of the device, which in this case is determined by the average reflectivity of the cell mirrors over the pulse bandwidth and the anti-reflection coatings of the plates, along with residual absorption or scattering inside the plate. Transmissions as high as 90% have been obtained in bulk plate-based nonlinear MPCs with careful optimization of the optical components.[21, 35, 36] In terms of group-velocity dispersion (GVD) engineering, both the cell mirrors and the choice of the bulk material can be used to adjust the average dispersion regime to the normal[21, 35, 36] or anomalous[34, 37] regime, allowing control over the nonlinear process.

When the pulse peak power to be manipulated is too high to result in controllable nonlinearity upon propagation in bulk materials (typically for femtosecond pulse peak power higher than 50 MW), the gas surrounding the MPC can be used to design the nonlinear properties, as detailed in next section.

2.3. Gas-filled nonlinear MPCs

The physics and design rules of gas-filled MPCs are quite different from MPCs including bulk plates, because the beam propagates in a homogeneously nonlinear medium. The fact that nonlinear phase is continuously accumulated while propagating over a distance that is comparable or larger than the Rayleigh range results in a larger robustness of the beam with respect to space-time couplings than when the B-integral can be considered to be accumulated in a single transverse plane, as is the case for bulk plate-based MPCs. An intuitive picture of this effect is that spatio-temporal components of the beam/pulse are simultaneously modified by the nonlinearity and mixed by diffraction, which homogenizes the spatio-temporal field. Because the beam remains in the nonlinear medium, the input peak power is strictly limited to the critical power $P_{crit} = 3.77\lambda_0^2/8\pi n_0 n_2$, where n_0 and n_2 are the linear and nonlinear indices of the gas at the pressure that is established around the MPC. However, since n_2 is proportional to the pressure, a large range of femtosecond pulse energies have been

accommodated by choosing the gas nature and pressure, from 100 µJ to 100 mJ. Gas-filled MPCs are typically operated at peak power levels between $0.2P_{crit}$ and $0.7P_{crit}$, to ensure a large enough B-integral per roundtrip while remaining well below the critical power. Most of the reported experiments have been aimed at pulse compression, and have therefore used atomic noble gases such as argon, krypton, or xenon, to avoid the Raman shift towards longer wavelength that is typically induced by molecular gases' nonlinear response. However, as was demonstrated recently in a number of experiments in gas-filled capillaries,[38, 39] molecular gases could be used to simultaneously perform spectral broadening and wavelength shifting of the input pulse.

The physical mechanism that prevents the growth of spatial degradation and spatio-temporal couplings when a pulse propagates through its focus in a homogeneous nonlinear medium was described by Milosevic and coauthors.[18] Starting from a fundamental Gaussian beam, they established using coupled-mode theory that, although the pulse couples some of its energy to higher order Laguerre-Gaussian modes when propagating towards its waist, the energy flow is reversed after the waist to restore a mostly Gaussian beam after the waist.

This can be interpreted in terms of a phase-mismatch due to the difference in accumulation of the Gouy phase between the fundamental and higher-order free-space modes. The Gouy phase associated to the propagation of a higher-order Laguerre-Gaussian beam is an integer multiple of the Gouy phase acquired by the fundamental Gaussian beam over the same path. Over a single pass through a focus, phase matching can therefore not be achieved, and energy transfer from the fundamental mode to higher-order modes is not efficient. However, a quasi-phase matching situation between the fundamental mode and a *p*-order mode can appear over several passes if the Gouy phase accumulated by the fundamental beam over one pass satisfies $\psi = \frac{n}{p}\pi$, with n=1,…, p-1. [22] These situations must be avoided since they result in a resonant energy transfer towards higher-order modes, and a rapid beam degradation. In

practice, most gas-filled MPC are operated in a near-concentric geometry corresponding to ψ approaching π, which makes this effect seldom observed: the level of nonlinearity that is necessary to couple a significant fraction of energy to a higher-order mode increases with the mode order.

The stability conferred by this mechanism to a Gaussian beam propagating in a nonlinear gas-filled MPC was investigated using numerical simulations,[40] and it was shown that it makes the beam quite robust, even at peak powers approaching the critical power. It explains the fact that experiments with a beam-averaged B-integral per roundtrip of up to 4.5 radians were conducted successfully.[41, 33] An illustration of this essential MPC property is given in **Figure 3**, where a simulated spatially resolved spectrum at the output of a nonlinear MPC is shown for a set of parameters corresponding to a mildly nonlinear MPC used for temporal compression. Parameters for this simulations are as follows: 300 fs 300 µJ input pulses at 1030 nm, propagating for 20 roundtrips in a MPC formed by two 300 mm radius of curvature mirrors separated by 500 mm and filled with 3 bars of argon. To quantify the spatio-spectral homogeneity experimentally, a metric *V* is often used. It is based on an overlap integral between the spectral intensity $I(\lambda)$ measured at a given location in the beam and a reference spectrum $I_0(\lambda)$, for example measured at the beam center:[36]

$$V = \left[\int \sqrt{I(\lambda) I_0(\lambda)}\, d\lambda\right]^2 / \left[\int I(\lambda) d\lambda \int I_0(\lambda) d\lambda\right]. \qquad (5)$$

This measurement only takes into account resemblance in terms of intensity, but full spatio-temporal electric field characterization in intensity and phase at the output of an MPC has confirmed that spatio-spectral or spatio-temporal couplings remain low even at high nonlinearity levels.[41]

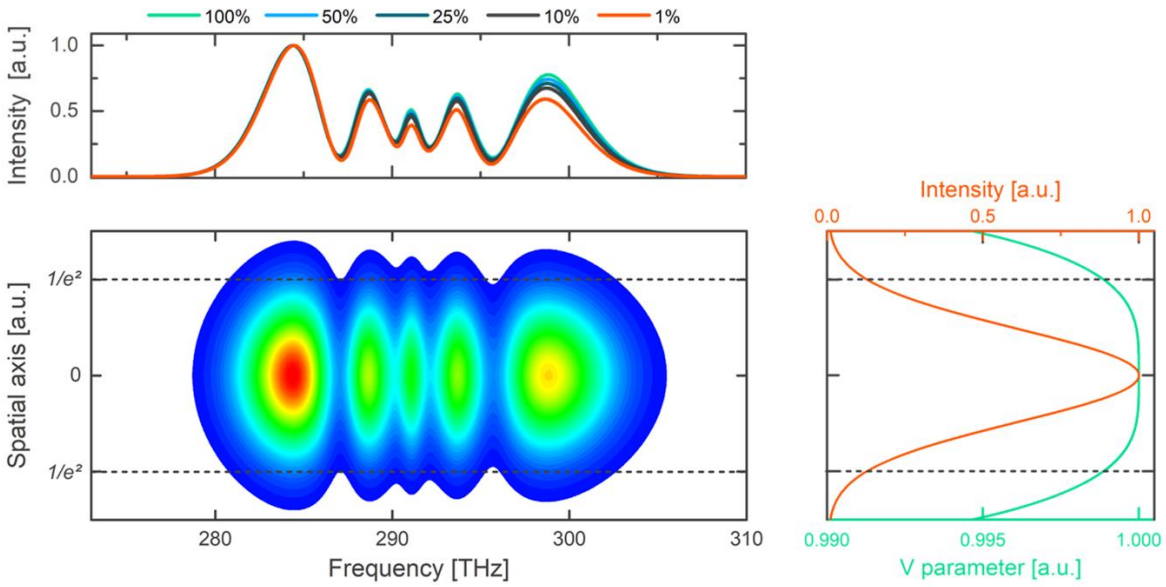

Figure 3. Simulated spatio-spectral beam structure at the output of a MPC with 20 roundtrips and a beam-averaged B-integral of 0.8 rad/roundtrip. Top: lineouts of the spectrum at various locations in the beam (X% in intensity), showing a mostly homogeneous profile. Right: integrated intensity profile and V parameter as a function of one transverse coordinate.

Analytical estimates for the stationary beam properties and accumulated B-integral that take into account nonlinear refraction to first order, in the aberrationless approximation, can be obtained by using a modified nonlinear Gaussian beam.[42] Kerr lensing due to the gas lowers both the stationary beam size at the waist and its divergence, resulting in a beam size at the waist given by

$$w_0 = \sqrt{\frac{\lambda L}{2\pi}\sqrt{\sigma\left(\frac{2R}{L}-1\right)}}, \qquad (6)$$

where $\sigma = 1 - P_{peak}/\sqrt{2}P_{crit}$ is the nonlinear correction term, assuming that the pulse temporal profile is Gaussian. If it is assumed that the pulse peak power is constant, this stationary beam propagation results in a roundtrip B-integral given by

$$B = \frac{8\pi n_0 n_2}{\lambda_0^2}\frac{P_{peak}}{\sqrt{\sigma}}\arctan\left(\sqrt{\frac{L}{2R-L}}\right). \qquad (7)$$

The design rules for energy scaling of gas-filled MPCs aimed at temporal compression can be outlined as follows: the input peak power limits the pressure for a given noble gas because of

the critical power for self-focusing. On the other hand, the MPC geometry is constrained by two phenomena, gas ionization at the MPC waist and damage at the mirrors. The latter often leads experimentalists to use near concentric cell geometries (*L* approaching *2R*), for which the beam size increases rapidly at the stability edge. However, this is accompanied by a decrease of the beam size at the waist, which is limited by ionization. If both limits cannot be alleviated simultaneously for a given radius of curvature of the mirror, both *R* and *L* must be increased. As a result, MPCs that are designed for high energy systems in the 100 mJ range are of the order of 10 m-long.[43] More quantitative discussion of energy scaling aspects can be found in references.[23, 28]

The GVD of noble gases in the visible and near infrared is normal, which can limit the spectral broadening if high pressures are used over large propagation distances, typically for moderate pulse energies in the range 100 µJ – 1 mJ. In this case, a compensating negative chirp can be introduced through engineering of the mirror coatings, as is done for bulk plate based MPCs. However, this same phenomenon usually results in smoother output spectra which translate in cleaner, improved contrast compressed pulses after chirp removal.[44]

2.4. Numerical simulations

Numerical simulations of the propagation in nonlinear MPCs have allowed both a deeper understanding of the physics at play and the design of specific experiments. In particular, it was used early on to assess the ability of MPCs to keep spatio-spectral or spatio-temporal couplings low enough for applications.[23] It continues to be an essential tool to test the potential of MPCs to be used in different contexts, such as with more exotic beams,[45, 46] to generate supercontinua,[47] or to understand the appearance of parasitic nonlinear effects such as four-wave mixing.[48] Depending on the problem parameters, a number of approaches with a wide range of computational complexity have been undertaken.

The most complete numerical simulations of the propagation are based on a three-dimensional description of the optical field *E(x,y,t)* propagating along the unfolded MPC axis *z*. Both generalized envelope equation[23] and unidirectional pulse propagation equation[47] approaches have been used. These models can capture the whole physical picture, including effects such as wavelength-dependent diffraction, the full dispersion characteristics, and nonlinear effects such as SPM, self-focusing, self-steepening, Raman scattering, and ionization and plasma-related effects. The specific reflectivity and dispersion properties of the cell mirror, that can play a crucial role in the dynamics, can be included easily. These 3D approaches allow to tackle the propagation of beams with arbitrary phase and intensity spatial and temporal profiles, such as Laguerre-Gaussian modes.[43, 45] However, they are quite demanding in terms of computation time, so that they are not ideal to describe simpler problems. In particular, when the temporal or spatial grid sizes must be expanded to accommodate for a temporally-stretched short pulse, or a highly divergent beam (in a near concentric MPC), the practicality of such models decreases quickly.

In a lot of situations, the beams that propagate in the nonlinear MPC possess radial symmetry, so that describing the field with a 2D function *E(r,t)* allows a full description of the propagation. In this case an efficient way to transform the field between the direct and frequency domains in space is to use the quasi-discrete Hankel transform,[49] while in the time domain the fast Fourier transform is used. This approach represents a good tradeoff whenever one wants to retain an accurate description of spatio-temporal couplings, e. g. to investigate a novel highly nonlinear MPC configuration. If the space-time structure of the beam is expected to be heavily influenced by the nonlinearity, for instance in MPCs where a Raman Stokes wave generation takes place,[50] this approach is also necessary.

However, if spatio-temporal couplings can be neglected, even simpler models that describe the field in the time domain *E(t)*, in a fashion similar to what is done in optical fibers, have been shown to be useful.[48, 41] In this case, the magnitude of the nonlinearity can be inferred

from a Gaussian beam parameter that is propagated over the same infinitesimal step dz as the field.[48] This allows to retain to first order the influence of Kerr lensing over the beam size and radius of curvature upon propagation in the MPC. Even simpler, the nonlinear parameter can be considered constant by averaging the beam size along the linear or nonlinear caustic described in Equation (1) or (6),[41] thereby obtaining an effective area. These models are much cruder than real spatio-temporal description of the propagation, but allow fast parameter scanning and can yield accurate results, e. g. in mildly nonlinear MPCs aimed at temporal compression. This particular application has triggered the development of nonlinear MPCs, and experimental results obtained in this context are reviewed in the next section.

3. Experimental implementations of temporal compression in MPCs

In nonlinear temporal compression experiments, input pulses are compressed by exploiting the spectral broadening induced by SPM in Kerr media.[4] If the nonlinear medium exhibits negligible or normal GVD, the spectrally broadened pulses must go through negative dispersion (using e. g. chirped mirrors) to be compressed close to their Fourier-transform limited duration. This technique has been known and used for decades, and was first implemented using liquid[51] or solid[52] nonlinear media in free-space propagation. The use of nonlinear waveguides as the Kerr medium became widespread because they allow a larger compression ratio due to the fixed spatial beam shape and long interaction length. In particular, solid core fibers[53, 54] and gas-filled capillaries[14] have been used for this purpose. In solid core fibers, self-focusing typically limits the input pulse energy to about 1 µJ for 1 ps duration. On the other hand, scaling rules for losses and nonlinearity in gas-filled capillaries restrict their use to the 100 µJ – 10 mJ range, although long, stretched, large core capillaries were very recently used at a 40 mJ energy level.[55] The 1 µJ – 100 µJ pulse energy gap can be filled using gas-filled large hollow core fibers such as Kagome[56] or antiresonant cladding designs.[57]

Nonlinear MPCs were recognized as an appealing technological alternative to waveguide for temporal compression with the first demonstration of their use in 2016.[21] Since then, a number of experiments have been reported in an energy range covering 1 µJ – 100 mJ, and input pulse durations in the 200 fs – 10 ps range, with compression ratios allowing to reach the few cycle regime. They have mostly been used in conjunction with high power femtosecond sources based on ytterbium doped materials: when combined, these technologies represent one of the most promising route towards future high average and peak power ultrafast laser systems. **Figure 4** summarizes the source performances obtained using temporal compression in MPCs on an output duration / output energy diagram. We now describe the salient features of a few noteworthy experiments.

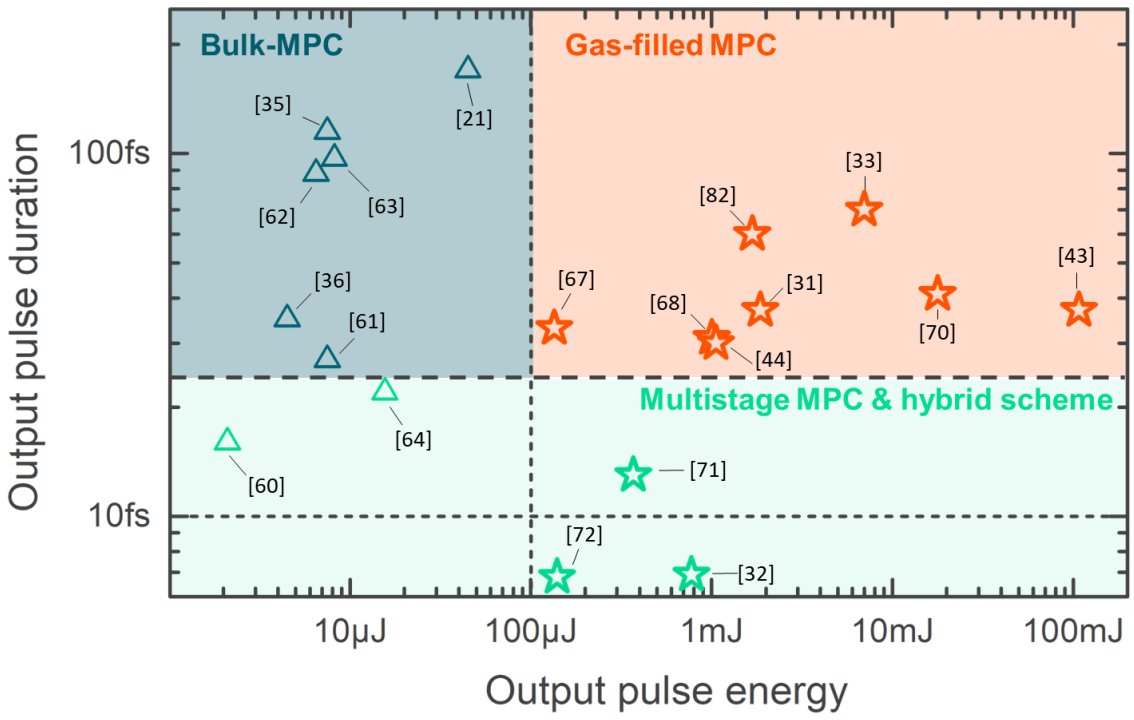

Figure 4. Summary of the experimental results obtained so far on a pulse energy – duration diagram.

3.1. Multipass cells including plates

Multipass cells including plates of a solid nonlinear medium were first demonstrated to compress pulses in the 1 – 100 µJ range, as an alternative to gas-filled hollow core fibers.

Indeed, these fibers can present drawbacks such as the lack of polarization maintaining properties, lack of robustness against beam pointing instabilities at high power or energy levels, or moderate throughput due to confinement losses. Multiple plates arrangements were first investigated as a way to limit spatio-temporal couplings in supercontinuum generation[16] or compression[17] experiments. They were quite successful in experiments where a low compression ratio is needed, for instance to compress short optical parametric chirped-pulse amplifiers (OPCPA)[17] or Ti:Sa-based laser sources[58] down to the few cycle regime. The extension of this concept to a nonlinear process distributed to an ever increasing number of plates,[59] to allow higher compression ratios, lead to nonlinear multipass cells including plates.

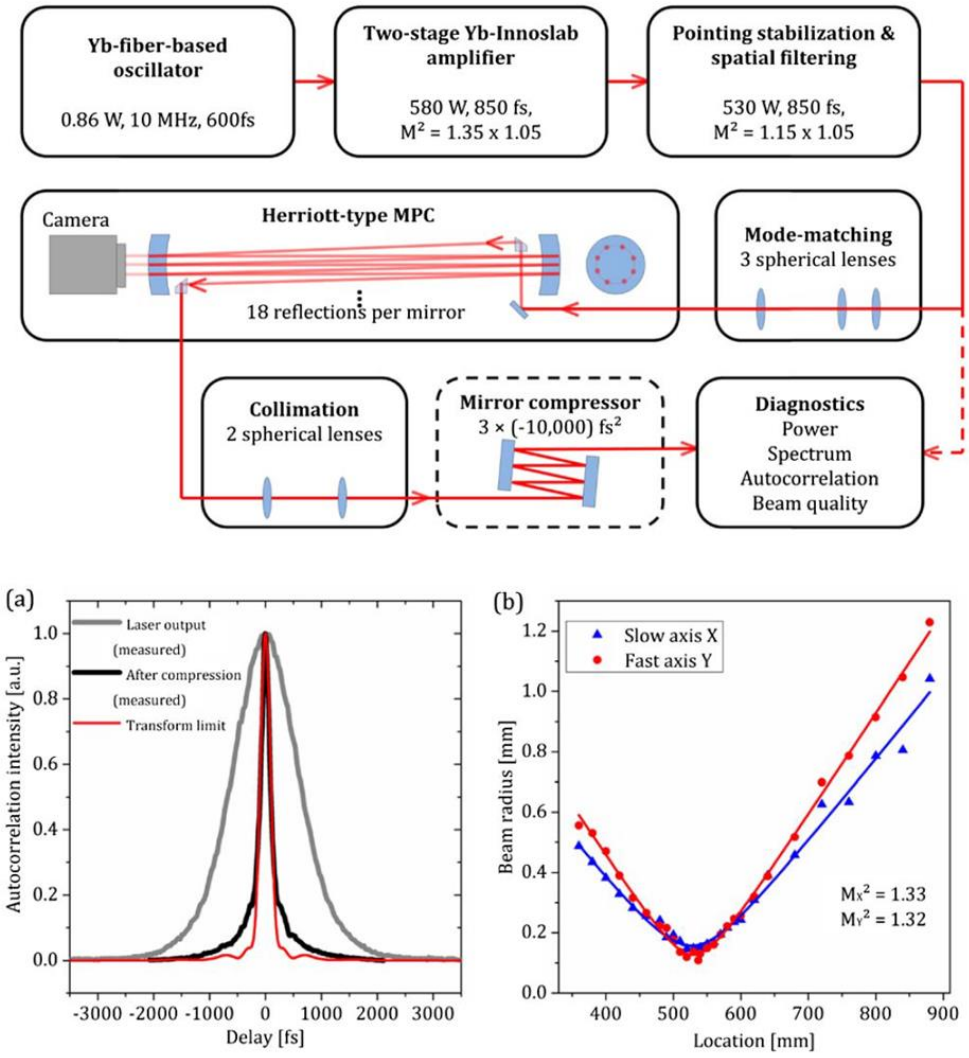

Figure 5. Top: Experimental setup corresponding to the first demonstration of pulse compression in a nonlinear MPC. The nonlinear elements inside the MPC are the fused silica substrates of the cell mirrors. Bottom: (a) Intensity autocorrelation traces measured at the input and output of the MPC. (b) Beam quality measurement at the output of the MPC. Adapted with permission. [21] Copyright 2016, The Optical Society.

The first demonstration of pulse compression in a nonlinear MPC is described in reference [21], illustrated in **Figure 5**. The laser source delivers 870 fs pulses at 40 µJ and a repetition rate of 10 MHz, corresponding to an average power of 400 W. These pulses are compressed in a Herriott cell where the end mirror substrates are AR coated on the inside and HR coated on the outside, so that pulses propagate in the substrate upon each reflection. An overall B-integral of 16 rad is accumulated over 18 roundtrips in the MPC, allowing compression down to 170 fs with a remarkable power throughput of 91%, and a near perfect beam quality. Decreasing peak power due to dispersion in the nonlinear medium can limit the spectral broadening in these systems. To circumvent this effect, an interesting design feature of this first experiment is that the dispersion of the substrates is compensated using engineered HR coatings on the MPC mirrors, already illustrating the design freedom allowed by MPCs. The very high average power also points out the robustness of the concept for power scaling. A final interesting point is that the input peak power is about ten times the critical power in the nonlinear material used, fused silica. Because the B-integral per pass is kept low, this has a negligible impact on the beam propagation in the MPC.

Since then a number of experiments were conducted on the same concept, with input energies as low as a few µJ[35, 36, 60] and repetition rates typically above 10 MHz. In particular, high energy thin disk oscillators perfectly fit this parameter range, and have been associated to nonlinear MPCs to decrease the pulse duration of Yb-doped crystals such as LuAG and YAG from >500 fs to <100 fs.[61, 62, 63] Although it was not the case in the first demonstration, the nonlinear medium is usually a plate located close to the MPC waist. Separating it from the substrate mirrors allows more design freedom, an easier replacement, and fine tuning of the

nonlinearity by moving it from the beam waist towards the cell mirrors. Cascading two bulk-based nonlinear MPC compression stages has allowed compression of 460 fs pulses down to 22 fs, corresponding to a compression ratio of 21, at 15 µJ output pulse energy.[64] Since the transmission of each stage is high, it is possible to use three stages to compress 220 fs pulses down to 16 fs, while maintaining a throughput of 60%, at an output pulse energy of 2.6 µJ.[60] Dispersion management and design of the cell mirrors is increasingly challenging as the output pulse duration decreases, especially because these MPC mirrors must be highly reflective to preserve a high transmission.

A recent experiment shows the benefits in associating a MPC-based pulse compression stage with a Nd:YVO_4 laser system emitting 10 ps pulses,[65] allowing compression down to 172 fs. In this case, a simpler laser technology, with very high gain materials, can be turned efficiently into a femtosecond source. Finally, a temporal compression setup based on a bulk nonlinear MPC was used in a carrier-envelope phase (CEP) stabilized system,[66] demonstrating the compatibility of both techniques despite the long beam path inside the cell.

3.2. Gas-filled multipass cells

At higher energy levels, gas-filled MPCs have been used in a number of experiments, almost exclusively with Yb-doped materials-based ultrafast laser sources. The whole cell is included in an airtight chamber filled with a noble gas at a controlled pressure.

To compress relatively low energy pulses in the 100 – 300 µJ range, MPCs are typically 50 cm-long, and are filled with a noble gas with a high nonlinearity such as xenon, krypton, or argon at pressures above the atmospheric pressure. One of the first demonstrations[67] showed compression of 160 µJ 275 fs pulses emitted at 150 kHz repetition rate by an Yb-doped fiber chirped pulse amplifier down to 33 fs, with 85% overall efficiency and perfect preservation of the input beam quality. The MPC chamber footprint was 45 cm × 20 cm.

As the pulse energy increases above 1 mJ, the MPC length must be increased to obtain larger beam diameters on the cell mirrors while allowing a sufficiently large beam waist to avoid ionization breakdown. To minimize the chamber footprint, a near-concentric geometry is often used, since it generally allows a more compact setup. The first demonstration of a gas-filled MPC was done with a 200 W average power, 2 mJ pulse energy Yb:YAG thin disk laser system delivering 210 fs pulses.[31] An originality of this work resides in the use of a 4f MPC geometry in lieu of the usual Herriott cell. This allows to tune the beam caustic in the MPC in terms of beam sizes, while keeping a stationary beam over one roundtrip. The setup allows compression of the output pulses down to 37 fs with a 93% efficiency. In this experiment, the MPC footprint is approximately 1.3 m × 1 m.

Scalability in terms of average power at the 1-10 mJ pulse energy level (using cell lengths of 1 – 2 m) was demonstrated by a number of experiments, with output power levels of 500 W, [44] 700 W,[33] and 1 kW,[68] with energy throughputs above 90% in all cases, and output pulse durations in the 30 – 70 fs range. The strategies followed to scale the average power that can be accommodated by nonlinear MPCs are not different than in other areas of photonics.[69] The heat deposited by high power beams in the materials and coatings is minimized by using very high reflectivity / low residual absorption and scattering components. This heat is then extracted from the system as efficiently as possible, e. g. using substrate materials with a high thermal conductivity and possibly water-cooling. The use of larger beam sizes on optical components such as cell mirrors, polarizers, and dispersion-compensating mirrors leads to lower thermal lenses and maximum temperatures, and reduces the possible influence of nonlinear absorption effects that appear in high average and peak power systems.

Scalability in terms of energy was demonstrated in two successive experiments by the same group, starting from an Yb:YAG thin disk laser system delivering 1.3 ps pulses at 5 kHz repetition rate and a pulse energy up to 200 mJ. The first experiment was made at 18 mJ energy.[70] It used a near concentric, 3 m-long cell filled with 600 mbar of argon, and resulted

in compression down to 41 fs. The second experiment used 110 mJ pulses launched in an 8 m-long cell filled with 0.25 bar of argon, and resulting in 37 fs output pulses.[43] The experimental setup and results of this work are reproduced in **Figure 6**. A very interesting technique is implemented in this second experiment: instead of using a standard Gaussian beam, the authors first convert it to a Laguerre-Gauss LG_{10} mode that features an orbital angular momentum with a topological charge of 1, using a spiral phase plate. This beam is launched inside the cell and undergoes SPM. At the output the beam is converted back to a Gaussian beam. The rationale for using such a beam is directly related to energy scaling. At a constant beam radius of curvature, the LG10 beam features a peak intensity that is 2.7 times less than a Gaussian beam, thereby avoiding the use of an even longer MPC. The LG_{10} beam features the same robustness as the Gaussian beam with respect to propagation in homogeneous nonlinear media. However, using even higher order beams to lower the intensity does not look as a possible route for energy scaling due to energy coupling to other higher order mode that are degenerate in terms of Gouy phase accumulation. In both these experiments, the output pulse compressibility was assessed using a fraction of the pulse energy, illustrating the technological difficulty to fabricate components such as chirped mirrors in large enough dimensions to withstand the full output peak power.

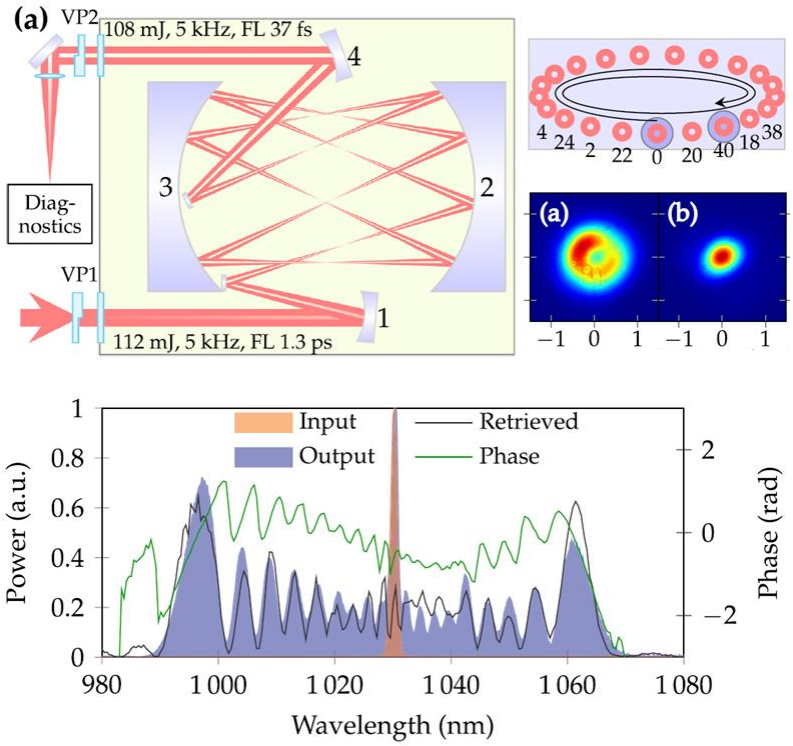

Figure 6. Top: Experimental setup corresponding to the record energy for pulse compression in a nonlinear MPC. A LG_{10} Laguerre-Gauss mode is used to decrease the peak intensity. Beam profile (a) shows the output of the MPC with no conversion plate back to a Gaussian beam, while (b) shows the output beam after the conversion plate. Bottom: Measured spectra at the input and output of the MPC, along with the output spectral phase. Adapted with permission. [43] Copyright 2021, The Optical Society.

The typical MPC-based compression experiment turns a few hundred fs pulse into a few tens fs pulse, with a ratio of around 10. To obtain larger compression ratios, for example to accommodate a longer input pulse duration, or venture into the few-cycle pulse regime, several stages can be cascaded. A remarkable result was obtained in this direction, where two MPCs are cascaded to compress 1.2 ps pulses down to 13 fs,[71] demonstrating a compression ratio of almost two orders of magnitude. However, one of the weaknesses of the MPC architecture is very apparent in this experimental result: enhanced metallic mirrors must be used in the second stage to accommodate the large bandwidth, which impairs both the energy scaling and throughput because of the large number of bounces required. As a result the output energy is 370 µJ, with an overall throughput of 37%.

To alleviate this drawback, a hybrid two-stage architecture was proposed[72] that takes advantage of the respective strengths of MPC- and capillary-based post-compression setups. A first MPC stage is used to reach a few tens of femtosecond, where highly efficient dielectric mirrors are available. The second stage uses a gas-filled capillary, with reduced losses because of the larger diameter that is permitted due to the first compression stage. Using this hybrid approach, the compression of 330 fs pulses down to 6.8 fs (two cycles at the central wavelength of 1030 nm) was demonstrated, with an overall efficiency of 61%. **Figure 7** illustrates the capability of this dual stage hybrid MPC/capillary setup to temporally compress pulses with a very high energy throughput, with a summary of the input and output spectral and temporal characteristics obtained at each stage in a recent implementation of this concept.

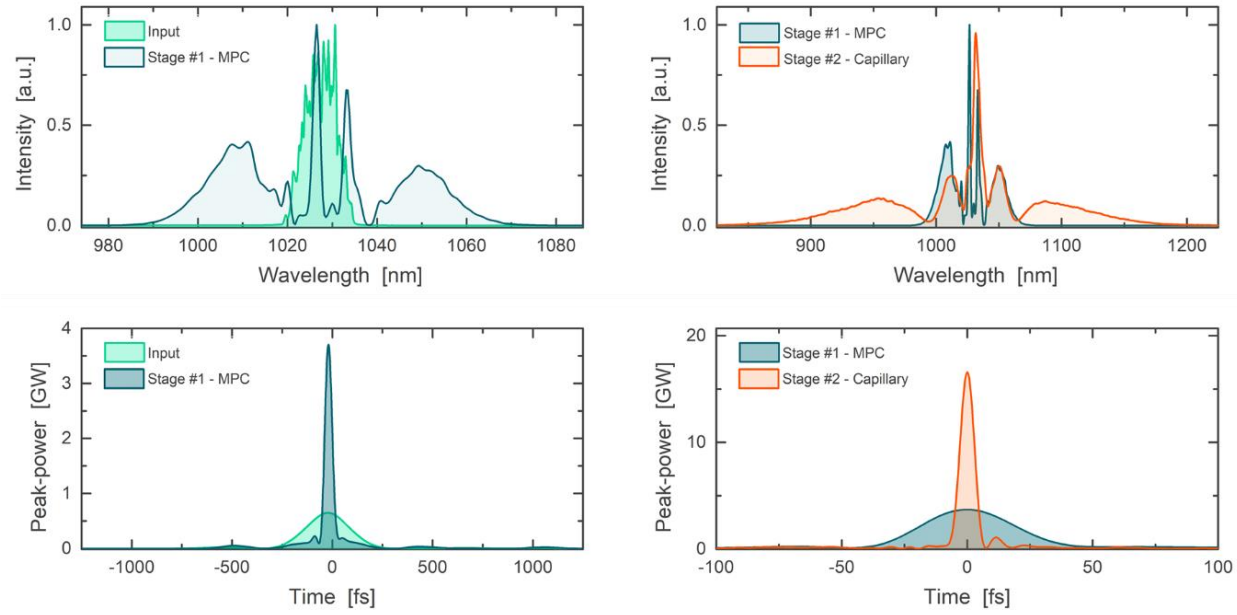

Figure 7. Left: gas-filled MPC-based compression stage, with an energy throughput of 90%. Right: Subsequent gas-filled capillary-based, with an energy throughput of 80%. Top: Optical spectra measured at the input and output of each stage. Bottom: Corresponding measured temporal profiles, with scale in instantaneous power. Based on a second implementation of the scheme described in reference.[72] The input laser delivers 200 µJ 260 fs pulses at 250 kHz, corresponding to 50 W average power. The output pulses exhibit a duration of 6.6 fs and an energy of 140 µJ.

Another method to reach few-cycle pulse durations at the output of MPC-based compressors with a high efficiency consists in designing a second MPC compression stage using enhanced

metallic mirrors with a small number of reflections.[32] Although the overall throughput could not be measured because only a fraction of the output power was sent to the chirped mirror compression system, the second MPC has a transmission of 82%, which is comparable to a capillary setup. Another interesting feature of this work is that the MPC is composed of multiple small curved mirrors instead of a single large-diameter mirror. Each mirror is fabricated on a silicon substrate and water-cooled, allowing an output average power of 388 W before the chirped mirrors, despite the non-optimal reflectivity of 98.5% of the metallic enhanced mirrors. This remarkable result shows that MPC-based setups can efficiently be used to reach the few-cycle regime at large average power.

3.3. Self-compression in multipass cells

Temporal compression experiments presented in the previous section were all done in a regime where the roundtrip-averaged GVD in the MPC is close to zero or normal. As a result, the peak power is either constant or slowly decreases inside the cell due to the interplay between nonlinearity and dispersion. The compression is really achieved at the output of the MPC, when negative dispersion is introduced to compensate for the SPM-induced positive chirp. When the average MPC dispersion is negative, however, soliton dynamics governs the evolution of the pulse,[10] resulting in an initial phase of temporal compression associated with spectral broadening inside the cell. This well-known phenomenon can be exploited to compress pulses without the need for chirp compensation at the output of the cell. Two experiments were reported that exploit this propagation regime, both using MPCs including a slab of fused silica. However the origin of the negative GVD differs.

The first experiment was done with 19 µJ 63 fs input pulses generated by an OPCPA at 1550 nm.[34] At this central wavelength, the dispersion of silica is anomalous, and since the cell mirrors are low-GVD, soliton dynamics occurs. As a result, the pulses are compressed down to 22 fs with a throughput of 73%, resulting in a 14 µJ output pulse energy. The compression

is clearly limited by the mirror dispersion and reflectivity bandwidth in this case, but the compressed pulse duration corresponds to four optical cycles.

The second experiment was performed with 12.8 µJ 300 fs pulses emitted from a high-energy Yb:YAG oscillator at 1030 nm.[37] The GVD of fused silica is positive at this wavelength, but the MPC mirror dielectric stacks were designed to introduce a negative dispersion that overcompensates the material dispersion over a roundtrip, so that the path-averaged GVD is anomalous. This results in output pulses compressed down to 31 fs with 11 µJ pulse energy. Compared to experiments done in the normal dispersion regime, the self-compression regime results in a peak power that varies drastically over propagation in the MPC, and the B-integral per roundtrip increases as the pulses self-compress. As a result, the process is less controlled, and, depending on the exact parameters, significant spatio-temporal couplings can occur. Moreover, as the soliton number increases, the output pulse temporal quality, e. g. defined in terms of the fraction of energy that is contained in the compressed pulse as opposed to a pedestal, decreases. As a consequence, this regime might not be the most appropriate for ultrafast laser development applications. However, the very rich soliton dynamics could be exploited for other purposes, such as wavelength conversion through soliton self-Raman scattering,[10] or supercontinuum generation[8, 47] at higher pulses energies than in optical fibers.

3. Other demonstrations of nonlinear effects in multipass cells

Although the focus application of nonlinear MPCs has clearly been temporal compression of high power / energy femtosecond linearly-polarized Gaussian beams, other uses have started to appear in recent years.

A first example is the compression of beams that are more complex than the fundamental Gaussian beam, either in terms of intensity and phase profile, or in terms of polarization state. Since light propagates in free space in a MPC, higher order modes and combinations thereof

can be used, and these possibilities start to be explored. One recent report[45] shows, using numerical simulations, the possibility to compress radially or azimuthally polarized beams, that can be described as combinations of orthogonally linearly polarized Hermite-Gaussian beams. The spatio-spectral homogeneity at the output is shown to be satisfactory up to a certain level of nonlinearity, in a behavior that is very similar to the one observed for standard beams. The same team investigated the possibility to compress Laguerre-Gaussian beams that carry an orbital angular momentum.[46] Their results shows the same robustness to spatio-temporal couplings than with fundamental Gaussian beams, especially for a topological charge equal to one. In fact, as explained earlier in the text, such beams were experimentally used in nonlinear MPCs,[43] not for their specific intensity and phase structure, but because their peak intensity is reduced compared to a conventional beam carrying the same pulse energy. These works show that it is probably only the beginning of nonlinear optics in MPCs exploiting the spatially multimode degree of freedom, much like nonlinear optics in multimode fibers has bloomed in recent years.[73]

Vectorial Kerr effects can also be used in MPCs, and a recent numerical work[74] is focused on the use of nonlinear ellipse rotation to enhance the temporal contrast of ultrashort pulses. It has been long known that when an elliptically polarized pulse propagates in a Kerr medium, cross-phase modulation results in an intensity-dependent rotation of the axes of the polarization ellipse. This phenomenon can be used to enhance the temporal contrast defined as the ratio of the peak power to the power of pre- or post-pulses, or to the power of a broad temporal pedestal.[75] Nonlinear ellipse rotation provides a nonlinear filtering action that has been used in capillaries[76] for contrast enhancement, and MPCs can also be used for this purpose in addition to pulse compression, albeit with tradeoffs between the achievable compression ratio, contrast enhancement, and energy efficiency.

Supercontinuum generation is another process that could benefit from the use of a nonlinear MPC. It was shown recently through numerical simulation that localized compressed blue-

shifted spatio-temporal wavepackets with extremely short durations can be obtained upon propagation in a MPC including a plate of nonlinear bulk material.[47] This phenomenon, similar to what has been previously observed in filamentation, is shown to be more efficient when the nonlinearity is distributed over a large number of passes in the MPC. Although experimental observations of such effects will probably be challenging because of the technical difficulties related to mirror coating design, this work suggests that complex nonlinear spatio-temporal phenomena could be advantageously performed and studied in MPCs.

Another recent example of a nonlinear process observed in a MPC is spectral compression.[77] This phenomenon is observed when negatively chirped pulses are subject to self-phase modulation. The nonlinear phase accumulated upon propagation shifts extreme spectral components towards the center of the spectrum, thereby cancelling the initial chirp and generating almost Fourier-transform limited pulses with an unchanged duration. Almost all such experiments have been done in fibers, at pulse energies limited by self-focusing to the µJ range. The use of a bulk material-based MPC, as previously observed for temporal compression, allows to use peak power in excess of the critical power, and to scale the energy of the spectrally compressed pulses.

Nonlinear MPCs are also used with nonlinear phenomena other than the Kerr effect. They were implemented as early as 1980 to extend the interaction length in Raman active gases to perform wavelength conversion of narrow bandwidth nanosecond pulses.[78,79,80] This idea was revisited recently to show that it is possible to transfer the energy of an input chirped femtosecond pulse to a long wavelength-shifted pulse through Raman stimulated scattering in a solid medium located in a MPC.[50] Here the use of a MPC brings a number of possible advantages compared to previous experiments done in single pass geometries through the material. It is possible to use higher peak powers, because the Raman material thickness is decreased in the multipass geometry. Recirculation inside the MPC provides a spatial filtering

action that results in near perfect beam quality of the Stokes generated beams. Finally, the MPC mirrors could be used to control the Raman cascade, for instance to optimize the conversion efficiency towards a given Stokes order.

As a final example of the rapid expansion of nonlinear phenomena observed in MPCs, several works report the generation of spectral content on the short-wavelength side of pulses that were meant to be compressed through self-phase modulation in gases.[44, 70] This generation appears at high nonlinearity level, and was interpreted as a four-wave mixing process that satisfies a quasi-phase matching relationship.[48] Although it was observed as a parasitic effect in pulse compression experiments, the periodic nature of the nonlinearity in MPCs offers phase matching opportunities that might be exploited to perform wavelength conversion through four-wave mixing, as was reported in gas-filled capillaries.[81]

4. Conclusion

To conclude, we have provided an overview on the use of MPCs as a platform for nonlinear optics experiments. These setups provide numerous engineering possibilities to control the nonlinear interactions, through the choice of MPC geometry, nonlinear media, and design of the cell mirrors. Taken as a whole, experiments on temporal compression described in section 3 clearly point to the future of high peak / high average power laser sources that will be necessary for societal applications of, e. g. laser-based particle accelerators. Scientific applications, for instance at free electron lasers installations, already take advantage of this method.[82] The most remarkable properties of MPCs in this context are their energy throughput, their extended free aperture that translates into a robustness to beam pointing and position fluctuations, and their power and energy scalability prospects. One of the key challenges for efficient implementation of this technique is mirror coating technology, in particular with the tradeoff between reflectivity, bandwidth, damage threshold and dispersion.

However, kW average power / TW peak power sources delivering pulses of 30 fs seem within grasp in the near future.

A number of other nonlinear physical phenomena and applications in photonics are being explored using MPCs, such as spectral compression, supercontinuum generation, contrast enhancement using nonlinear elliptical polarization rotation, wavelength conversion using stimulated Raman scattering. In addition, the use of beam structures that are more complex than a linearly polarized Gaussian beam are starting to appear, notably radially or azimuthally polarized beams, or beams carrying orbital angular momentum. Future work will undoubtedly continue to expand the range of applications of MPCs as a platform for nonlinear optics. The robustness of these setups with respect to spatio-temporal couplings at reasonable nonlinearity levels makes MPCs a sort of extension of optical fibers, a privileged geometry to study and use nonlinear optics in science and engineering.

Acknowledgements
This work was supported by the following grants: Agence Nationale de la Recherche (ANR) (ANR-10-LABX-0039-PALM, ANR-16-CE30-0027-01-HELLIX, ANR-19-CE30-0001-02-MIRTHYX). Conseil départemental de l'Essonne (ASTRE SOPHIE).

Conflict of Interest
The authors declare no conflict of interest.

Received: ((will be filled in by the editorial staff))
Revised: ((will be filled in by the editorial staff))
Published online: ((will be filled in by the editorial staff))

References

[1] R. Boyd, *Nonlinear optics*, 3rd edition, Academic Press **2008**.

[2] M. Müller, A. Klenke, T. Gottschall, R. Klas, C. Rothhardt, S. Demmler, J. Rothhardt, J. Limpert, A. Tünnermann, *Opt. Lett.* **2017**, *42*, 2826.

[3] G. Cerullo, S. De Silvestri, *Rev. Sci. Instr.* **2003**, *74*, 1.

[4] T. Nagy, P. Simon, L. Veisz, *Advances in Physics: X* **2021**, *6*, 1845795.

[5] B. R. Washburn, J. A. Buck, S. E. Ralph, *Opt. Lett.* **2000**, *25*, 445.

[6] A. Jullien, O. Albert, F. Burgy, G. Hamoniaux, J.-P. Rousseau, J.-P. Chambaret, F. Augé-Rochereau, G. Chériaux, J. Etchepare, N. Minkovski, S. M. Saltiel, *Opt. Lett.* **2005**, *30*, 920.

[7] S. Kinoshita, H. Ozawa, Y. Kanematsu, I. Tanaka, N. Sugimoto, S. Fujiwara, *Rev. Sci. Instr*. **2000**, *71*, 3317.

[8] J. M. Dudley, G. Genty, S. Coen, *Rev. Mod. Phys.* **2006**, *78*, 1135.

[9] F. Krausz, M. Ivanov, *Rev. Mod. Phys.* **2009**, *81*, 163.

[10] G. P. Agrawal, *Nonlinear fiber optics*, 5th edition, Academic Press **2012**.

[11] F. Stutzki, F. Jansen, H.-J. Otto, C. Jauregui, J. Limpert, A. Tünnermann, *Optica* **2014**, *1*, 233.

[12] F. Couny, F. Benabid, P. S. Light, *Opt. Lett.* **2006**, *31*, 3574.

[13] B. Debord, A. Amsanpally, M. Chafer, A. Baz, M. Maurel, J. M. Blondy, E. Hugonnot, F. Scol, L. Vincetti, F. Gérôme, F. Benabid, *Optica* **2017**, *4*, 209.

[14] M. Nisoli, S. De Silvestri, O. Svelto, R. Szipöcs, K. Ferencz, C. Spielmann, S. Sartania, F. Krausz, *Opt. Lett.* **1997**, *22*, 522.

[15] A. Mysyrowicz, A. Couairon, U. Keller, *New J. Phys.* **2008**, *10*, 025004.

[16] C.-H. Lu, Y.-J. Tsou, H.-Y. Chen, B.-H. Chen, Y.-C. Cheng, S.-D. Yang, M.-C. Chen, C.-C. Hsu, A. H. Kung, *Optica* **2014**, *1*, 400.

[17] C.-H. Lu, T. Witting, A. Husakou, M. J. Vrakking, A. H. Kung, F. J. Furch, *Opt. Expr.* **2018**, *26*, 8941.

[18] N. Milosevic, G. Tempea, T. Brabec, *Opt. Lett.* **2000**, *25*, 672.

[19] N. V. Vysotina, N. N. Rosanov, V.E. Yashin, *Optics and Spectroscopy* **2011**, 110, 973.

[20] S. N. Vlasov, E. V. Koposova, V. E. Yashin, *Quant. Electron.* **2012**, *42*, 989.

[21] J. Schulte, T. Sartorius, J. Weitenberg, A. Vernaleken, P. Russbueldt, *Opt. Lett.* **2016**, *41*, 4511.

[22] P. Russbueldt, J. Weitenberg, A. Vernaleken, T. Sartorius, J. Schulte, U.S. 9847615, **2017**.

[23] M. Hanna, X. Délen, L. Lavenu, F. Guichard, Y. Zaouter, F. Druon, P. Georges, *J. Opt. Soc. Am. B* **2017**, *34*, 1340.

[24] D. Herriott, H. Kogelnik, R. Kompfner, *Appl. Opt.* **1964**, *3*, 523.

[25] D. R. Herriott, H. J. Schulte, *Appl. Opt.* **1965**, *4*, 883.

[26] D. Kaur, A. M. de Souza, J. Wanna, S. A. Hammad, L. Mercorelli, D. S. Perry, *Appl. Opt.* **1990**, *29*, 119.

[27] A. Sennaroglu, J. G. Fujimoto, *Opt. Express* **2003**, *11*, 1106.

[28] R. M. Kaumanns, *Ph.D. thesis*, Ludwig-Maximilians-Universität München **2020**.

[29] A. E. Siegman, *Lasers*, Univ. Science Books, revised edition **1986**.

[30] M. A. Bouchiat, L. Pottier, *Appl. Phys. B* **1982**, *29*, 43.

[31] M. Ueffing, S. Reiger, M. Kaumanns, V. Pervak, M. Trubetskov, T. Nubbemeyer, F. Krausz, *Opt. Lett.* **2018**, *43*, 2070.

[32] M. Müller, J. Buldt, H. Stark, C. Grebing, J. Limpert, *Opt. Lett.* **2021**, *46*, 2678.

[33] P. L. Kramer, M. K. R. Windeler, K. Mecseki, E. G. Champenois, M. C. Hoffmann, F. Tavella, *Opt. Express* **2020**, *28*, 16951.

[34] G. Jargot, N. Daher, L. Lavenu, X. Delen, N. Forget, M. Hanna, P. Georges, *Opt. Lett.* **2018**, *43*, 5643.

[35] J. Weitenberg, T. Saule, J. Schulte, P. Rußbüldt, *IEEE J. Quant. Elec.* **2017**, *53*, 8600204.

[36] J. Weitenberg, A. Vernaleken, J. Schulte, A. Ozawa, T. Sartorius, V. Pervak, H.-D. Hoffmann, T. Udem, P. Russbüldt, T. W. Hänsch, *Opt. Express* **2017**, *25*, 20502.

[37] S. Gröbmeyer, K. Fritsch, B. Schneider, M. Poetzlberger, V. Pervak, J. Brons, O. Pronin, *Appl. Phys. B* **2020**, *126*, 159.

[38] J. E. Beetar, M. Nrisimhamurty, T.-C. Truong, G. C. Nagar, Y. Liu, J. Nesper, O. Suarez, F. Rivas, Y. Wu, B. Shim, M. Chini, *Sci. Adv.* **2020**, *21*, eabb5375.

[39] P. A. Carpeggiani, G. Coccia, G. Fan, E. Kaksis, A. Pugžlys, A. Baltuška, R. Piccoli, Y.-G. Jeong, A. Rovere, R. Morandotti, L. Razzari, B. E. Schmidt, A. A. Voronin, A. M. Zheltikov, *Optica* **2020**, *7*, 1349.

[40] M. Ueffing, *Ph. D. thesis*, Ludwig-Maximilians-Universität München, **2018**.

[41] N. Daher, F. Guichard, S. W. Jolly, X. Délen, F. Quéré, M. Hanna, P. Georges, *J. Opt. Soc. Am. B* **2020**, *37*, 993.

[42] M. Hanna, L. Daniault, F. Guichard, N. Daher, X. Délen, R. Lopez-Martens, P. Georges, *OSA Continuum* **2021**, *4*, 732.

[43] M. Kaumanns, D. Kormin, T. Nubbemeyer, V. Pervak, S Karsch, *Opt. Lett.* **2021**, *46*, 929.

[44] P. Russbueldt, J. Weitenberg, J. Schulte, R. Meyer, C. Meinhardt, H. D. Hoffmann, R. Poprawe, *Opt. Lett.* **2019**, *44*, 5222.

[45] H. Cao, R. S. Nagymihaly, V. Chvykov, N. Khodakovskiy, M. Kalashnikov, *J. Opt. Soc. Am. B* **2019**, *36*, 2517.

[46] H. Cao, R. S. Nagymihaly, M.Kalashnikov, *Opt. Lett.* **2020**, *45*, 3240.

[47] C. Mei, G. Steinmeyer, *Phys. Rev. Research* **2021**, *3*, 013259.

[48] M. Hanna, N. Daher, F. Guichard, X. Délen, P. Georges, *J. Opt. Soc. Am. B* **2020**, *37*, 2982.

[49] M. Guizar-Sicairos, J. C. Gutiérrez-Vega, *J. Opt. Soc. Am. A* **2004**, *21*, 53.

[50] N. Daher, X. Délen, F. Guichard, M. Hanna, P. Georges, *Opt. Lett.* **2021**, *46*, 3380.

[51] R. A. Fisher, P. L. Kelley, T. K. Gustafson, *Appl. Phys. Lett.* **1969**, *14*, 140.

[52] C. Rolland, P. B. Corkum, *J. Opt. Soc. of Am. B* **1988**, *5*, 641.

[53] B. Zysset, W. Hodel, P. Beaud, H. P. Weber, *Opt. Lett.* **1986**, *11*, 156.

[54] B. Nikolaus and D. Grischkowsky, *Appl. Phys. Lett.* **1983**, *42*, 1.

[55] G. Fan, P. A. Carpeggiani, Z. Tao, G. Coccia, R. Safaei, E. Kaksis, A. Pugzlys, F. Légaré, B. E. Schmidt, A. Baltuška, *Opt. Lett.* **2021**, *46*, 896.

[56] F. Guichard, A. Giree, Y. Zaouter, M. Hanna, G. Machinet, B. Debord, F. Gérôme, P. Dupriez, F. Druon, C. Hönninger, E. Mottay, F. Benabid, P. Georges, *Opt. Express* **2015**, *23*, 7416.

[57] F. Köttig, F. Tani, P. St. J. Russell, *Opt. Lett.* **2020**, *45*, 4044.

[58] M. Stanfield, N. F. Beier, S. Hakimi, H. Allison, D. Farinella, A. E. Hussein, T. Tajima, and F. Dollar, *Opt. Express* **2021**, *29*, 9123.

[59] C.-H. Lu, W.-H. Wu, S.-H. Kuo, J.-Y. Guo, M.-C. Chen, S.-D. Yang, A. H. Kung, *Opt. Express* **2019**, *27*, 15638.

[60] K. Fritsch, M. Poetzlberger, V. Pervak, J. Brons, O. Pronin, *Opt. Lett.* **2018**, *43*, 4643.

[61] C.-L. Tsai, F. Meyer, A. Omar, Y. Wang, A.-Y. Liang, C.-H. Lu, M. Hoffmann, S.-D. Yang, C. J. Saraceno, *Opt. Lett.* **2019**, *44*, 4115.

[62] F. Meyer, N. Hekmat, T. Vogel, A. Omar, S. Mansourzadeh, F. Fobbe, M. Hoffmann, Y. Wang, C. J. Saraceno, *Opt. Express* **2019**, *27*, 30340.

[63] F. Meyer, T. Vogel, S. Ahmed, C. J. Saraceno, *Opt. Lett.* **2020**, *45*, 2494.

[64] E. Vicentini, Y. Wang, D. Gatti, A. Gambetta, P. Laporta, G. Galzerano, K. Curtis, K. McEwan, C. R. Howle, N. Coluccelli, *Opt. Express* **2020**, *28*, 4541.

[65] J. Song, Z. Wang, R. Lu, X. Wang, H. Teng, J. Zhu, Z. Wei, *Appl. Phys. B* **2021**, *127*, 50.

[66] M. Natile, A. Golinelli, L. Lavenu, F. Guichard, M. Hanna, Y. Zaouter, R. Chiche, X. Chen, J. F. Hergott, W. Boutu, H. Merdji, P. Georges, *Opt. Lett.* **2019**, *44*, 3909.

[67] L. Lavenu, M. Natile, F. Guichard, Y. Zaouter, X. Delen, M. Hanna, E. Mottay, P. Georges, *Opt. Lett.* **2018**, *43*, 2252.

[68] C. Grebing, M. Müller, J. Buldt, H. Stark, J. Limpert, *Opt. Lett.* **2020**, *45*, 6250.

[69] S. Hädrich, J. Rothhardt, S. Demmler, M. Tschernajew, A. Hoffmann, M. Krebs, A. Liem, O. de Vries, M. Plötner, S. Fabian, T. Schreiber, J. Limpert, A. Tünnermann, *Appl. Opt.* **2016**, *55*, 1636.

[70] M. Kaumanns, V. Pervak, D. Kormin, V. Leshchenko, A. Kessel, M. Ueffing, Y. Chen, T. Nubbemeyer, *Opt. Lett.* **2018**, *43*, 5877.

[71] P. Balla, A. Bin Wahid, I. Sytcevich, C. Guo, A.-L. Viotti, L. Silletti, A. Cartella, S. Alisauskas, H. Tavako, U. Grosse-Wortmann, A. Schönberg, M. Seidel, A. Trabattoni, B. Manschwetus, T. Lang, F. Calegari, A. Couairon, A. L'Huillier, C. L. Arnold, I. Hartl, C. M. Heyl, *Opt. Lett.* **2020**, *45*, 2572.

[72] L. Lavenu, M. Natile, F. Guichard, X. Délen, M. Hanna, Y. Zaouter, P. Georges, *Opt. Express* **2019**, *27*, 1958.

[73] K. Krupa, A. Tonello, A. Barthélémy, T. Mansuryan, V. Couderc, G. Millot, P. Grelu, D. Modotto, S. A. Babin, S. Wabnitz, *APL Photonics* **2019**, *4*, 110901.

[74] V. Pajer, M. Kalashnikov, *Laser Phys. Lett.* **2021**, *18*, 065401.

[75] K. Sala and M. C. Richardson, *J. Appl. Phys.* **1978**, *49*, 2268.

[76] N. Smijesh, X. Zhang, P. Fischer, A. A. Muschet, R. Salh, A. Tajalli, U. Morgner, L. Veisz, *Opt. Lett.* **2019**, *44*, 4028.

[77] N. Daher, F. Guichard, X. Délen, Y. Zaouter, M. Hanna, P. Georges, *Opt. Express* **2020**, *28*, 21571.

[78] W. R. Trutna, R. L. Byer, *Appl. Opt.* **1980**, *19*, 301.

[79] R. Saint-Loup, B. Lavorel, G. Millot, C. Wenger, H. Berger, *J. Raman Spectrosc.* **1990**, *21*, 77.

[80] R. Sussmann, T. Weber, E. Riedle, H. J. Neusser, *Opt. Comm.* **1992**, *88*, 408.

[81] F. Belli, A. Abdolvand, J. C. Travers, P. St. J. Russell, *Opt. Lett.* **2019**, 44, 5509.

[82] A.-L. Viotti, S. Alisauskas, A. Bin Wahid, P. Balla, N. Schirmel, B. Manschwetus, I. Hartl, C. M. Heyl, *J. Synchrotron Radiat.* **2021**, *28*, 36.

We review the principles, experimental implementations, and applications of nonlinear optics in multipass cells. This platform allows distribution of the nonlinear interaction over large distances and multiple beam foci. We focus on the main application of these systems, post-compression of femtosecond pulses, while also providing a broader picture of the physics and application possibilities.

Marc Hanna*, Florent Guichard, Nour Daher, Xavier Délen, Patrick Georges

Nonlinear optics in multipass cells